Validation of ^{55}Mn(n,2n) and ^{127}I(n,2n) LWR spectrum averaged differential cross sections

Nicola Burianová[1], Michal Košťál[1], Martin Schulc[1], Jan Šimon[1], Martin Mareček[1], Jan Uhlíř[1]

[1]Research Centre Řež, Husinec – Řež, 25068

Keywords: Cross section measurement; Nuclear data; Reactor dosimetry; LR-0 reactor; ^{55}Mn(n,2n) reaction; ^{127}I(n,2n) reaction

Abstract

The article describes the measurement of ^{55}Mn(n,2n) and ^{127}I(n,2n) reaction rates in a well-defined reactor spectrum. The reaction rates are derived from gamma activities of irradiated MnO_2 and NaI samples by measuring them at HPGe detector. The spectral average cross section in ^{235}U prompt fission neutron spectrum was experimentally determined to be 0.2393 ± 0.042 mb for ^{55}Mn and 1.2087 ± 0.043 mb for ^{127}I.

The experimental values of cross sections are compared with calculations by MCNP6 code using ENDF VII.1, ENDF VII, JEFF-3.1, JEFF-3.2, JENDL-3.3, JENDL-4, ROSFOND- 2010, CENDL-3.1 and IRDFF nuclear data libraries. The measured cross section of ^{55}Mn is with good agreement with ENDF VII.1, JEFF 3.1, JENDL 3.3, JENDL 4, ROSFOND and CENDL 3.1 nuclear data libraries, where C/E-1 is 0.1%, while IRDFF under predict by about 15.8%. The ^{127}I measurement shows more significant discrepancies. With good agreement is ENDF VII.1, ENDF VII and ROSFOND nuclear data libraries, where C/E-1 is 2.0%, but JENDL 3.3 and JENDL 4 over predicts the result by about 31.3%.

1 Introduction

The process of neutron induced cross sections verification is ongoing under the auspices of the International Atomic Energy Agency (IAEA). The measurement of spectrum-average cross section for selected reactions is of high interest since they are used for the reactor dosimetry, where these reactions are used for monitoring neutron flux. The presented neutron cross sections are derived from experimental reaction rates that are evaluated from the measured gamma activities of the activation product by HPGe (High Purity Germanium) detector. The experimental reaction rates are compared with the reaction rates calculated using various nuclear data libraries and various descriptions of prompt fission neutron spectra. The correction to the spectral shift caused by the relatively thick target geometry and capsule mounting is employed and evaluated by Monte Carlo (MC) calculation.

2 LR-0 reactor

The irradiation experiment was performed in a special core assembled in the LR-0 reactor. It is a zero power, light water pool type reactor operated by the Research Center Rez (Czech Republic). The LR-0 reactor was originally designed for the research of the pressurized water reactor (PWR) physics (VVER type cores). A multi-purpose design of the technological equipment allows carrying out experiments on VVER-1000 or VVER-440 type assemblies and with small modifications also on PWR type. The reactor works at atmospheric pressure and room temperature. Continuous nominal power is 1 kW. Criticality is reached by filling the reactor tank with moderator, which is pure demineralized water, to the critical height, H_{cr}.

Reactor core in this experiment consist of six uranium fuel assemblies and dry central channel with NaI and MnO_2 capsules. One fuel assembly contains 312 fuel elements and 18 stainless steel tubes for shut down or control clusters. An illustration of the LR-0 reactor and a scheme of the core configuration for this experiment are shown in the Figure **1**. Fuel assemblies are assembled of shortened VVER-1000 elements (sintered UO_2 pellets, outer diameter 7.53 mm, central inner hole 1.4

mm, active length 125 cm, total length 135.7 cm, Zr cladding tube with the outer diameter of 9.15 mm, wall thickness 0.72 mm).

The power monitoring channels positions are indicated in the Figure **1** by round circles around the core. The distances of these eight dry channels to the closest fuel pin, indicated by subscripts “a” to “l”, are measured perpendicularly to the fuel assembly wall. The fuel enrichment for each assembly can be also seen in the Figure **1**.

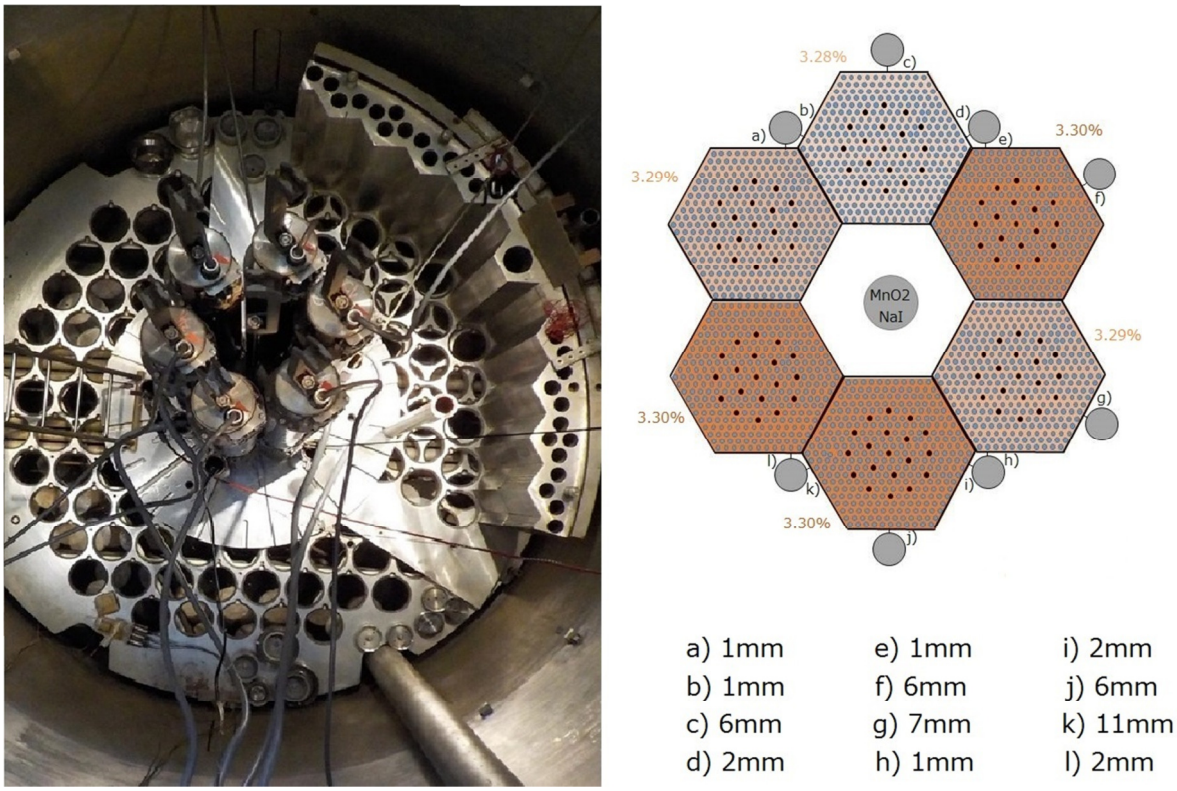

Figure 1: Overhead view at LR-0 reactor core (left) and radial plot of the core with position of irradiated sample (right).

3 Experimental and calculation methods

3.1 Irradiation arrangement

The studied ^{55}Mn and ^{127}I was in the form of encapsulated MnO_2 and NaI. Both capsules were placed in dry channel in the center of LR-0 core onto each other. This special core was designed for IRDFF testing because it was already well-defined and characterized by reactivity Kostal et al. 2016, fission rates distribution by Kostal et al. 2016, neutron spectrum Kostal et al. 2017 and also by flux distribution in cavity center Kostal et al. 2018. MnO_2 and NaI were used because the chosen materials have the suitable neutronic properties, which are reflected by the spectral shift correction factor.

$Mn0_2$ and NaI were fed into aluminum capsule with inner diameter 8 cm and external diameter 8.2 cm, which is the same diameter as HPGe detector. The bottom of Mn capsule was placed in 22.4 cm above the zero fuel level and the critical height of the moderator during this experiment was 56.06 cm during the first day of irradiation and 56.09 cm during the second day (see the Figure **2**).

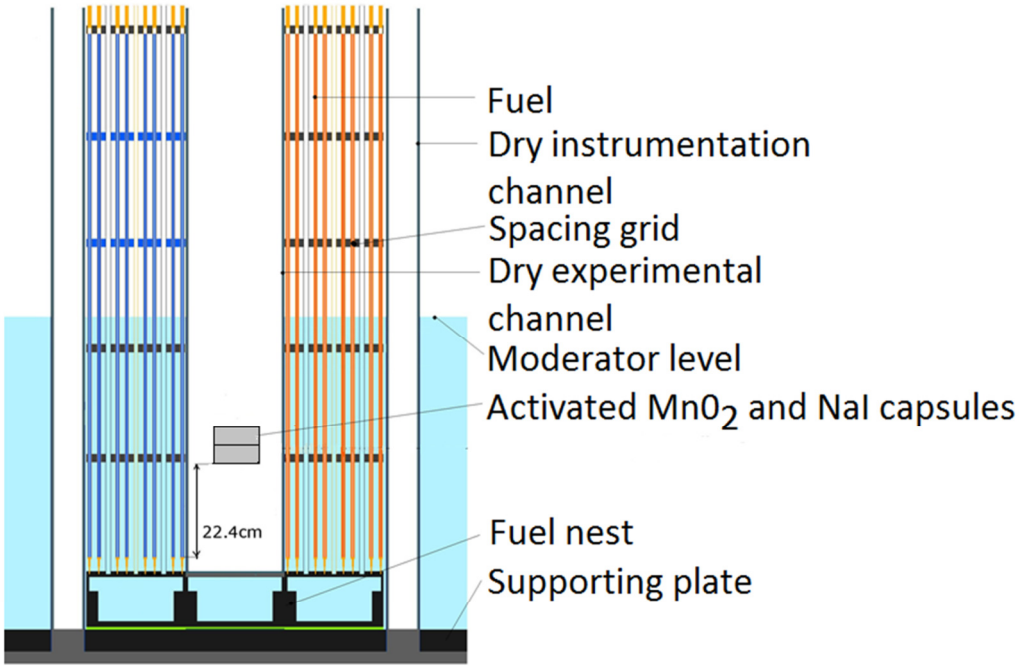

Figure 2: Axial view of the reactor core with irradiated capsules.

The irradiation was carried out 13 hours (7 hours first day and 6 hours second day of irradiation). The relative power evolution is plotted in the Figure **3**. Reference time for subsequently evaluation was chosen as the end of irradiation the second day.

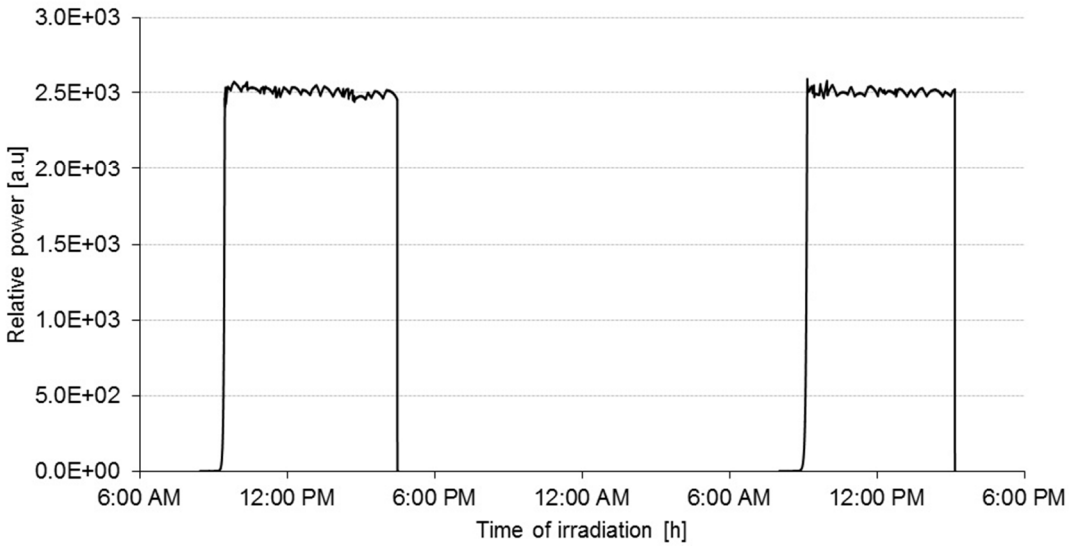

Figure 3: Reactor power during the irradiation.

The activation foils were located in the defined positions on the outer surface of both capsules – radially symmetric positions (Au in 60° symmetry and Ni in 120°symmetry). Foils of Au and Ni were placed in the middle of bottom and around both capsules (1.15 cm above the capsule bottom at MnO_2 and 3.2 cm above the bottom at NaI capsule), see the Figure **4**. The thickness of capsules bottom was 3 mm and cap was 1.5 mm thick. The density of MnO_2 capsule was 1.626 g/cm^3 and weight was 99.68 g. NaI sample had density 2.144 g/cm^3 and weight 143.32 g. The height of MnO_2 in capsule was 1.22 cm and height of NaI in aluminum capsule was 1.33 cm. A set of 1% Au and 100% Ni foils were used for both relative measurement of reaction rate gradient and flux monitoring.

The reaction rates of radioisotopes originating during an irradiation period can be described by the equation:

$$\frac{A(\overline{\mathrm{P}})}{A_{\mathrm{Sat}}(\overline{\mathrm{P}})} = \sum P_{\mathrm{rel}}^{i}\left(1 - e^{-\lambda.T_{\mathrm{Irr}}^{i}}\right)e^{-\lambda.T_{\mathrm{end}}^{i}}, \qquad (1)$$

where

$\frac{A(\overline{P})}{A_{\mathrm{Sat}}(\overline{P})}$; is relative portion of saturated activity induced during irradiation experiment

P_{rel}^{i}; is relative power on i-th interval in irradiation, $P_{\mathrm{rel}}^{i} = \frac{P^{i}}{\overline{\mathrm{P}}}$

T_{ir}^{i}; is irradiation time on i-th interval in irradiation

T_{end}^{i}; is time from end of i-th interval in to reference time (end of irradiation)

λ ; is decay constant

$\overline{\mathrm{P}}$; is average power

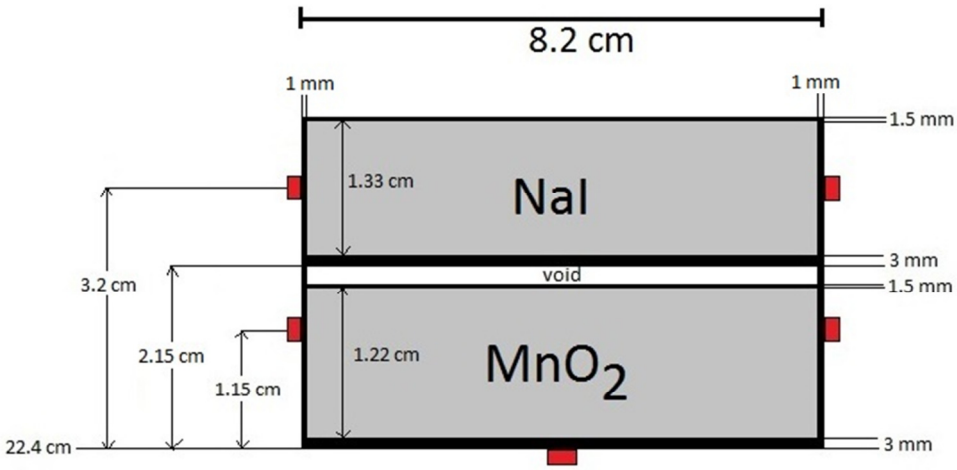

Figure 4: The diagram of MnO_2 and NaI capsules and positions of activation foils (red rectangles).

3.2 HPGe spectrometry

Gamma spectrometry was used for determination of capsules activity by Net Peak Area (NPA). For measuring was used HPGe (High Purity Germanium, Ortec GEM35P4) detector placed in lead shielding with a thin inner copper lining covered with rubber for suppression of a background signal. Each capsule was measured directly at the top face of the detector (the detector diameter is approximately equal to capsule diameter), see the Figure **5**. The HPGe detector efficiency calibration was calculated by MCNP6 code. The computing model of detector was compiled using experimentally determined parameters of detector, which were measured from detector radiogram and precisely measured dead layer (similarly to Dryak and Kovar 2006). The detector model was verified with the point etalon and Marinelli beaker sources. The discrepancy between calculation and experiment in relevant gamma energy region is about 1.9% in the point source, which is identical with foils measurement and 1% in Marinelli beaker geometry, which is close to the capsules measurement. The energy calibration was performed using the standard point sources ^{60}Co, ^{88}Y, ^{137}Cs, ^{152}Eu and ^{241}Am with an uncertainty less than 1.0 keV throughout the energy range used, as shown in

the Figure **6**. The NPA was also corrected to coincidences by coincidence summing correction factor (CSCF) Tomarchio et al. 2009 .

The obtained photon spectrum was analyzed by Genie 2000 software (Canberra). This program analyzed required peaks and calculated their NPA, which was used in equation (2) for determination of reaction rate as $C(T_m) = NPA/t$, where *t* is a live time of sample measurement.

The uncertainty of count rates, which makes at most 1.3% includes the following main components: the gross peak area, the Compton continuum area, the background area and the parameters in the energy and peak shape calibrations. The detector efficiency uncertainty, being about 1% for volume source and about 1.9% for point source, covers statistical uncertainty of gamma transport from source to HPGe, uncertainty in Marinelli beaker position and uncertainty of source distribution in volume source is determined as bias between calculated and experimentally determined efficiency. Besides above stated uncertainties, there are also other stochastic uncertainties: the radionuclide half-time value, the pin radial or axial position data determination and the reactor shut-down time uncertainties. However, these uncertainties are negligible in comparison with the count rate uncertainties.

Parameters of measured nuclides are summarized in Table **1**.

Table 1: Summary of measured gamma peaks from irradiated capsules.

Reaction	^{55}**Mn(n,2n)**	^{127}**I(n,2n)**	
Gamma line [keV]	834.8	388.6	666.3
Detector efficiency	1.80E-02	2.94E-02	2.01E-02
Branching ratio [%]	99.98	35.60	32.90
A/A_{sat}	1.21E-3	2.83E-2	
$T_{1/2}$ [d]	312.20	12.93	
Spectral shift correction	1.048	1.009	
CSCF	1	0.997	

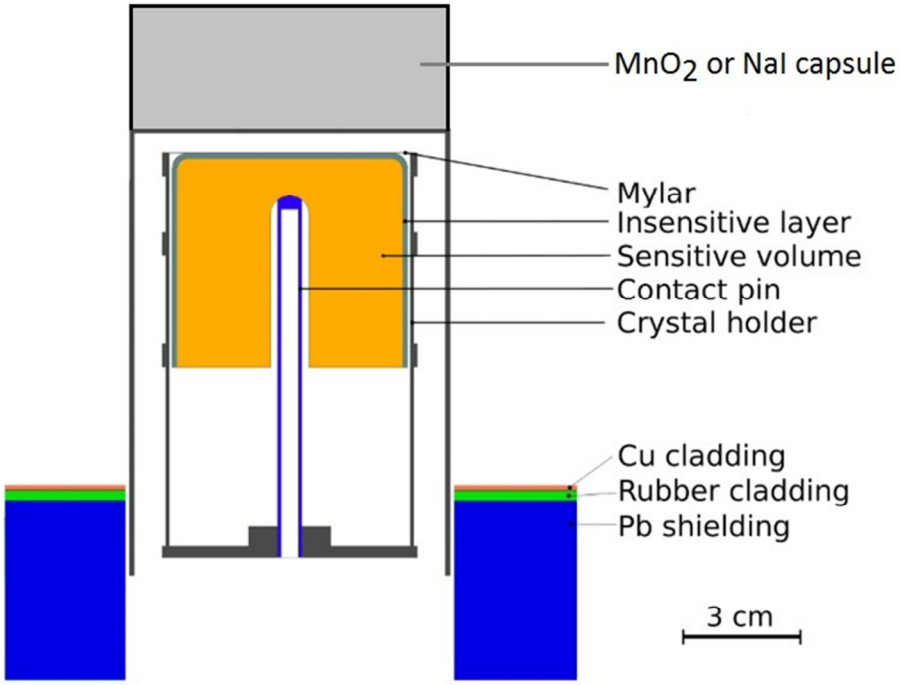

Figure 5: The scheme of HPGe detector with irradiated capsule at the end cup and with the scheme of detector shielding.

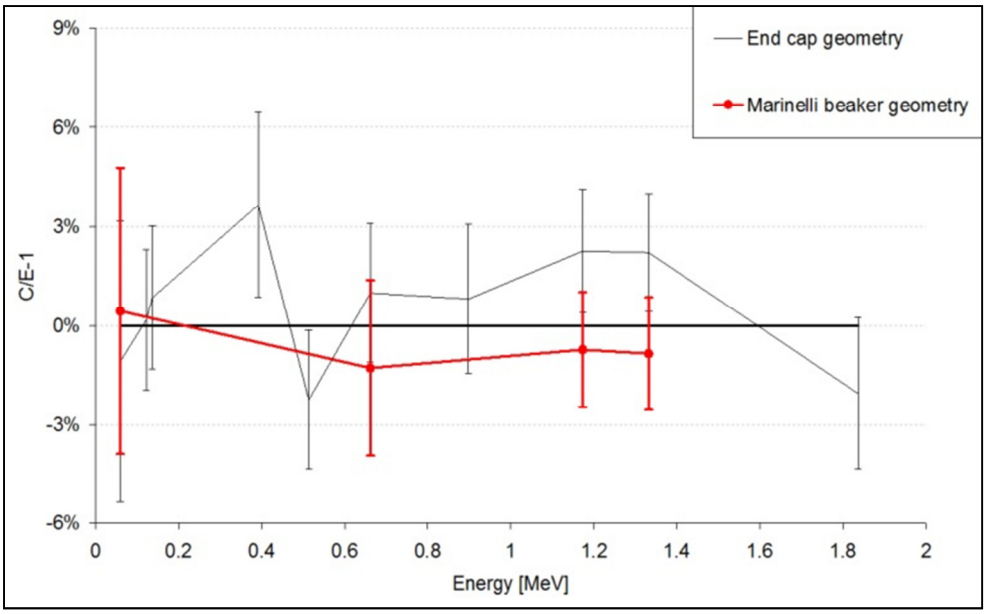

Figure 6: Validation of used HPGe detector in both measured geometries.

3.3 Evaluation of (n,2n) reaction cross-section

The integral cross sections are derived from the reaction rates of the samples scaled to unit neutron emission rate. The scaling factors normalizing measurement to actual irradiation power, used in evaluation of ^{55}Mn(n,2n) and ^{127}I(n,2n) reaction rates, have been determined by reaction rates derived from gamma activity of activation foils. Two kinds of foils were used: 1% Au in Al and 100% Ni. Foil were cylindrical with 3.6 mm diameter and thickness of 0.1 mm. Irradiated activation foil was placed in a plastic cover of EG3 point source type – outer diameter 25 mm and inner diameter 4 mm and also measured at the end cup the detector. For Au foils the spectrum was evaluated for the 411.8 keV peak of ^{198}Au originating from the ^{197}Au(n,γ) reaction and for Ni foil the spectrum was evaluated for the 810.8 keV peak of ^{58}Co originating from the ^{58}Ni(n,p) reaction. Parameters of foils are summarized in Table **2**. The measurement of foils started immediately after the end of irradiation.

The self-absorption in foils and the geometry corrections were negligible as well as correction to the dead time. The reaction rate during irradiation was determined using equation (2):

$$q = \left(\frac{A_{\mathrm{Sat}}(\overline{\mathrm{P}})}{A(\overline{\mathrm{P}})} \right) C(\mathrm{T}_m) \frac{\lambda}{\varepsilon \eta N} \frac{1}{\left(1 - e^{-\lambda.\mathrm{T}_m}\right)} \frac{1}{e^{-\lambda.\Delta\mathrm{T}}}, \qquad (2)$$

where:

q ; is the reaction rate of activation during power density $\overline{\mathrm{P}}$ (power in first day of irradiation experiment);

T_m ; is live time of measurement by HPGe;

$\Delta\mathrm{T}$; is the time between the end of irradiation and the start of HPGe measurement;

$\mathrm{C}(\mathrm{T}_m)$; is the measured number of counts;

$\mathcal{E}$; is the gamma branching ratio;

η ; is the detector efficiency (the result of MCNP6 calculation);

N ; is the number of target isotope nuclei;

The experimental reaction rate of the studied (n,2n) reactions were scaled to unit neutron emission in the core using the scaling factor K derived from the monitoring activation foils. The scaling factor *K* was determined from the comparison of calculated and measured reaction rates of the activation foils. It is worth nothing that the average scaling factors determined from Au and Ni is approximately 4.20E+11 for ^{55}Mn and also for ^{127}I. The assumed uncertainty in determined scaling factor is about 3.5%. The scaling factor used for absolute neutron flux evaluation can be described by equation:

$$K = \frac{K_{\mathrm{Au}} + K_{\mathrm{Ni}}}{2}, \tag{3}$$

where

$K_{\mathrm{Au}} = \sum_{i=1}^{N} \frac{q_{\mathrm{Au}}^{i}(1\,\mathrm{nps})_{\mathrm{Calculated}}}{q_{\mathrm{Au}}^{i}(\overline{\mathrm{P}})_{\mathrm{Measured}}}$ is the scaling factor determined from the Au reaction rates

$K_{\mathrm{Ni}} = \sum_{i=1}^{N} \frac{q_{\mathrm{Ni}}^{i}(1\,\mathrm{nps})_{\mathrm{Calculated}}}{q_{\mathrm{Ni}}^{i}(\overline{\mathrm{P}})_{\mathrm{Measured}}}$ is scaling factor determined from Ni reaction rates.

Table 2: Summary of activation detectors parameters.

Activation material	^{198}Au	^{58}Co
Reaction	^{197}Au(n,γ)	^{58}Ni(n,p)
Gamma line [keV]	411.8	810.8
Branching ratio [%]	95.62	99.45
$T_{1/2}$ [days]	2.6947	70.86
A/A_{sat}	1.20E-1	5.31E-3
Detector efficiency	8.30E-02	4.63E-02
Derived Reaction Rate	4.43E-15	2.79E-18
CSCF	0.998	0.936
K	4.05E+11	4.37E+11

The simulations of neutron and photon transport were performed in criticality calculations using MCNP6 Monte Carlo code and ENDF/B-VII.0 (Chadwick et al. 2006) data library. Simulation of gamma transport from the sample to the HPGe detector was determined with a single gamma transport model. Simulation of target activation caused by neutron transport in it was determined in critical model. More details can be found in Kostal et al. 2017b.

For purposes of the extension of IRDFF database, the SACS of both reactions in ^{235}U was derived from the SACS of reactions averaged in LR-0 spectrum (see Eq. 4) using spectral shift correction factor. That is determined calculationally as a ratio between the spectral-averaged cross section in the full geometry used and the spectral-averaged cross section in ^{235}U prompt fission neutron spectrum (PFNS). The spectral shift correction factor includes all effects of core components on ^{235}U PFNS, contribution of ^{235}U PFNS and also the effect of the relatively thick target and capsule material on reactor spectra in the central cavity. The effect of the capsule components on neutron spectrum was determined calculationally in the isotopic ^{235}U field. The statistical uncertainties of Monte Carlo calculations of the reaction rates are in all cases below 1.3% while fission source uncertainty is about 0.2%.

$$\overline{\sigma}_{E>10MeV}^{\mathrm{exp.}} = \frac{1}{K}\frac{q}{\int_{\mathrm{E}>10\,\mathrm{MeV}} \varphi(\mathrm{E})d\mathrm{E}}\mathrm{C}, \tag{1}$$

where K is the scaling factor based on absolute flux density, neutron emission per second, $\varphi(\mathrm{E})$ is the calculated neutron spectrum normalized per 1 neutron in core and C is the correction factor to the spectral shift effect.

4 Results

The summary of measured results is in Table **3**. Notable discrepancies were found in ^{127}I(n,2n) cross section. JENDL 3.3 and JENDL 4 over predict the result by about 31.3%. ROSFOND, ENDF VII and ENDF VII.1 results differ from experiment by 2%. Less discrepancies were found in ^{55}Mn(n,2n) cross section, see Table **5**.

The components of the total uncertainty are listed in Table **4**. Because the sources of uncertainties are assumed as not-correlated, the total uncertainty is derived as square root of the sum of the squares of all combined uncertainties.

Table 3: Results of MnO_2 and NaI measurement.

	^{55}Mn(n,2n)	**^{127}I(n,2n)**
A [Bq]	8.046493	453.8715
q [1/s]	5.13E-21	2.78E-20
Neutron emission rate [1/s]	4.2E+11	4.2E+11
Sample correction to spectral shift in capsule [-]	1.047913	1.008727
SACS in LR-0 reactor spectra >10 MeV [mb]	163.6019	858.4357
Cross section in ^{235}U [mb]	0.2393	1.2087
Uncertainty	4.2%	4.3%

Table 4: Uncertainties of NaI and $Mn0_2$ measurement.

	^{127}I(n,2n)	**^{55}Mn(n,2n)**
Statistical uncertainty in gamma spectrometry measurement	1.10E-02	1.02E-02
Bias between evaluated peaks	1.06E-02	-
Statistical uncertainty in Au foils measurement	1.13%	
Statistical uncertainty in Ni foils measurement	1.75%	
Bias between Au and Ni foils based scaling factors	2.6%	
Uncertainty in spectral shift correction	1%	1%
Uncertainty in HPGe description for samples (Figure **6**)	1.9%	
Uncertainty in HPGe description for activation foils measurement	1%	
Total uncertainty	4.3%	4.2%

Table 5: Calculation and C/E-1 comparison with ^{55}Mn(n,2n) and ^{127}I(n,2n) reaction rates experimental data.

	^{55}Mn(n,2n)			**^{127}I(n,2n)**		
	Calculated RR [s-1]	C/E-1	Uncertainty	Calculated RR [s-1]	C/E-1	Uncertainty
ENDF VII.1	5.13E-21	0.1%	0.229	2.73E-20	-2.0%	1.174
ENDF VII	4.93E-21	-3.9%	0.219	2.73E-20	-2.0%	1.174
JEFF 3.2	5.48E-21	6.8%	0.244	2.97E-20	6.6%	1.277
JEFF 3.1	5.13E-21	0.1%	0.229	2.97E-20	6.6%	1.277
JENDL 3.3	5.13E-21	0.1%	0.229	3.66E-20	31.3%	1.573
JENDL 4	5.13E-21	0.1%	0.229	3.66E-20	31.3%	1.573
ROSFOND	5.13E-21	0.1%	0.229	2.73E-20	-2.0%	1.174
CENDL 3.1	5.13E-21	0.1%	0.229	3.09E-20	11.1%	1.331
IRDFF	4.32E-21	-15.8%	0.192	2.69E-20	-3.5%	1.157

5 Conclusion

The ^{55}Mn(n,2n) and ^{127}I(n,2n) cross sections were derived from measured data. The resulting cross sections averaged across the ^{235}U spectrum is 0.2393 ± 0.042 mb in case of ^{55}Mn(n,2n) reaction and 1.2087 ± 0.043 mb in case of ^{127}I(n,2n) reaction. The cross section of ^{55}Mn is with a good agreement with most of libraries except IRDFF, where the value is under predict by about 15.8% and JEFF 3.2 where the value is over predict by about 6.8%. The ^{127}I measurement shows notable discrepancies with most of libraries. With good agreement are ROSFOND, ENDF VII.1 and ENDF VII nuclear libraries which under predict the measured result by about 2%. JENDL 3.3 and JENDL 4 libraries over predict the result by about 31.3%.

6 Acknowledgement

The presented work was financially supported by the Ministry of Education, Youth and Sport Czech Republic Project LQ1603 (Research for SUSEN). This work has been realized within the SUSEN Project (established in the framework of the European Regional Development Fund (ERDF) in project CZ.1.05/2.1.00/03.0108).

References

Capote et al. 2012 R. Capote, K.I. Zolotarev, V.G. Pronyaev, and A. Trkov, Journal of ASTM International (JAI)- 9, Issue 4, 2012, JAI104119

Capote et al. 2016 “Prompt Fission Neutron Spectra of Actinides”, Nucl. Data Sheets 131 (2016) 1–106

Chadwick et al. 2006 M.B. Chadwick, P. Obložinský, M. Herman et al ENDF/B-VII.0: Next Generation Evaluated Nuclear Data Library for Nuclear Science and Technology, Nucl. Data Sheets, **107**, 2006, pp. 2931-3060, ISSN 0090-3752,

Chadwick et al. 2011. M.B. Chadwick, M. Herman, P. Obložinský et al, "ENDF/B-VII.1: Nuclear Data for Science and Technology: Cross Sections, Covariances, Fission Product Yields and Decay Data", Nucl. Data Sheets, **112,** (2011), pp. 2887–2996

Chadwick et al. 2014 “The CIELO Collaboration: Neutron Reactions on ^{1}H, ^{16}O, ^{56}Fe, 235;238U, and 239Pu”, Nucl. Data Sheets 118, 1–25 (2014).

CMI 2011 http://www.eurostandard.cz/Eurostandard-catalog-2011.pdf

Dryak and Kovar 2006 P. Dryak, P. Kovar, Experimental and MC determination of HPGe detector efficiency in the 40–2754 keV energy range for measuring point source geometry with the source-to-detector distance of 25 cm, Appl. Rad. and Isot., Vol. 64, Issues 10–11, 2006, pp. 1346-1349

Ge et al 2010. Z.G. Ge, Y.X. Zhuang, T.J. Liu, J.S. Zhang, H.C. Wu, Z.X. Zhao, H.H. Xia, The Updated Version of Chinese Evaluated Nuclear Data Library (CENDL-3.1), Proc. International Conference on Nuclear Data for Science and Technology, Jeju Island, Korea (April 2010), pp. 26–30
Goorley et al. 2012 T. Goorley, et al., "Initial MCNP6 Release Overview", Nuclear Technology, **180**, pp 298-315 (Dec 2012).
Koning et al. 2006 A.J. Koning, R. Forrest, M. Kellett et al., "The JEFF-3.1 Nuclear Library, JEFF Report 21," NEA No. 6190 (2006)
Koning et al. 2010 A.J. Koning, et al. "Status of the JEFF Nuclear Data Library", Proceedings of the International Conference on Nuclear Data for Science and Technology, Jeju Island, Korea, 2010, p.1057
Kostal et al. 2016 Michal Košťál, Vojtěch Rypar, Ján Milčák, Vlastimil Juříček, Evžen Losa, Benoit Forget, Sterling Harper, Study of graphite reactivity worth on well-defined cores assembled on LR-0 reactor, Ann. of Nucl. En., Vol. 87, 2016, pp. 601-611, ISSN 0306-4549
Kostal et al. 2016a Michal Košťál, Marie Švadlenková, Petr Baroň et al, Determining the axial power profile of partly flooded fuel in a compact core assembled in reactor LR-0, Annals of Nuclear Energy, Vol. 90, 2016, pp. 450-458, ISSN 0306-4549,
Kostal et al. 2017 M. Košťál, Z. Matěj, F. Cvachovec, V. Rypar, E. Losa, J. Rejchrt, F. Mravec, M.Veškrna, Measurement and calculation of fast neutron and gamma spectra in well defined cores in LR-0 reactor, Appl. Rad. and Isot., Vol. 120, 2017, pp 45-50
Kostal et al. 2017b M. Košťál, M. Schulc, V. Rypar, E. Losa, N. Burianová, J. Šimon, M. Mareček, J.Uhlíř, Validation of zirconium isotopes (n,g) and (n,2n) cross sections in a comprehensive LR-0 reactor operative parameters set, In Appl. Rad. and Isot., Vol. 128, 2017, Pp 92-100, ISSN 0969-8043
Kostal et al. 2017c On similarity of various reactor spectra and ^{235}U Prompt Fission Neutron Spectrum, M. Košťál, Z. Matěj, E. Losa et al, will be published
Kostal et al. 2018 M. Košťál, M. Schulc, J. Šimon, N. Burianová, D. Harutyunyan, E. Losa, V. Rypar, Measurement of various monitors reaction rate in a special core at LR-0 reactor, In Ann. of Nucl. En., Vol. 112, 2018, Pp 759-768, ISSN 0306-4549
Shibata et al. 2002 K. Shibata, T. Kawano, T. Nakagawa, et al., Japanese Evaluated Nuclear Data Library Version 3 Revision-3: JENDL-3.3, Journal of Nuclear Science and Technology, 39 (2002), p. 1125
Shibata et al. 2011 K. Shibata, O. Iwamoto, T. Nakagawa, N. Iwamoto, A. Ichihara, S. Kunieda, S. Chiba, K. Furutaka, N. Otuka, T. Ohsawa, T. Murata, H. Matsunobu, A. Zukeran, S. Kamada, J. Katakura, JENDL-4.0: A new library for nuclear science and engineering, J. Nucl. Sci. Technol., 48 (2011), pp. 1–30
Tomarchio et al. 2009 E. Tomarchio, S.Rizzo, Coincidence-summing correction equations in gamma-ray spectrometry with p-type HPGe detectors, Radiation Physics and Chemistry, Vol. 80 (2011), pp. 318–323
Zabrodskaya et al. 2007 S. Zabrodskaya, A. Ignatyuk, V. Kosheev, M. Nikolaev, V. Pronyaev, ROSFOND – Russian national library of neutron data VANT (Voprosi Atomnoy Nauki i Techniki) Ser. Nucl. Const., 1–2 (2007), pp. 3–21
Zsolnay et al. 2012 E.M.Zsolnay, R. Capote, H.K. Nolthenius, and A. Trkov, Technical report INDC(NDS)-0616, IAEA, Vienna, 2012.